

Published in final edited form as:

J Am Chem Soc. 2012 April 4; 134(13): 5798–5800. doi:10.1021/ja211601k.

Europium(III) DOTA-tetraamide complexes as redox active MRI sensors

S. James Ratnakar[†], Subha Viswanathan[†], Zoltan Kovacs^{†,‡}, Ashish K. Jindal[†], Kayla N. Green[†], and A. Dean Sherry^{†,‡,*}

[†]Advanced Imaging Research Center, University of Texas Southwestern Medical Center, 5323 Harry Hines Boulevard, Dallas, Texas, 75390

[‡]Department of Chemistry, University of Texas, Dallas, 800 West Campbell Road, Richardson, Texas, 75080

Abstract

PARACEST redox sensors containing the NAD⁺/NADH mimic *N*-methylated quinolinium moiety as redox active functional group have been designed and synthesized. The Eu³⁺-complex with two quinolinium moieties was nearly completely silent in CEST in the oxidized form, but “turns on” upon reduction with β-NADH. The CEST effect of the Eu³⁺- complex containing only one quinolinium group was much less redox responsive but showed an unexpected sensitivity to pH in the physiologically relevant pH range.

Keywords

PARACEST; Redox; Europium; MRI

Proper regulation of the cellular redox state is critical to many fundamental biochemical processes. Localized changes in the redox potential have been shown to play an important role in signal transduction influencing a wide variety of cellular functions.¹ Despite its biological significance, currently there is no convenient non-invasive method to map the ambient redox potential in living tissues. Magnetic resonance imaging (MRI) is a powerful noninvasive diagnostic tool and promising results have been achieved in the development of various redox sensitive Gd³⁺ and Mn^{2+/3+} based (shortening) contrast agents.^{2–4} Over the past decade, chemical *T*₁ exchange saturation transfer (CEST) agents have evolved as a viable alternative to traditional (*T*₁) agents, especially in the adaptation of MRI to molecular imaging.^{5,6} DOTA-tetraamide complexes of paramagnetic hyperfine shifting Ln³⁺-ions, in particular Eu³⁺, induce large paramagnetic shifts of the metal bound water protons and have sufficiently slow water exchange rates to satisfy the slow to intermediate exchange condition ($k_{ex} \leq \Delta\omega$) for CEST.^{6,7}

It has been demonstrated that comparatively small changes in the structure of the coordinating amide side arms of Eu³⁺-DOTA tetraamide complexes can generate large changes in the frequency and/or magnitude of the CEST effect originating from the metal bound water molecule.^{8–10} Our approach to develop redox sensitive MRI agents relies on this sensitivity of the CEST signal on the water exchange rate.¹¹ By attaching one or more

Corresponding Author dean.sherry@utsouthwestern.edu, Phone 214 645 2730; fax 214 645 2744.

Supporting Information Available: The synthetic procedure, experimental details, ¹H NMR spectroscopy, CEST spectra as a function of applied *B*₁, CEST fitting data, and electrochemical data. This material is available free of charge via the Internet at <http://pubs.acs.org>

redox active group to the coordinating pendant arms of a Eu^{3+} -chelate, the redox status of the reporter group should have a detectable influence on the CEST signal. We have shown previously that the oxidized and reduced form of a Eu^{3+} -DOTA-tetraamide containing a *p*-nitrophenylamide functionality could be discriminated by CEST spectroscopy and MR imaging.⁸ However, this complex cannot be used as an *in vivo* redox sensor because the redox potential of this system is outside the biologically relevant range. Our design for a potentially biocompatible redox active CEST agent is based on the reversible redox reactivity of the nicotinamide moiety in the nicotinamide adenine dinucleotide (NAD^+/NADH) coenzyme system.^{12,13} Several nicotinamide, quinoline and acridine derivatives have been reported that are capable of mimicking the function of NAD^+/NADH . While the pyridinium/1,4-dihydropyridine redox systems are the closest analogs to the NAD^+/NADH , these compounds are extremely susceptible to degradation in aqueous solutions. Quinoline derivatives are significantly more stable and still display reasonable reactivity in biomimetic reductions.¹⁴ Our hypothesis was that reduction of the quinolinium moiety to the dihydroquinoline derivative would induce a sufficient change in the coordination environment around the lanthanide ion to modulate the water exchange lifetime of the Eu^{3+} bound water molecule. Using these principles, we have designed and synthesized two Eu^{3+} -DOTA-tetraamide complexes (Eu^{3+} -(**1**) and Eu^{3+} -(**2**), Figure 1) containing one or two quinolinium groups attached to the pendant arm of the DOTA-tetraamide moiety, respectively. The ligands were synthesized by alkylating the *tert*-butyl esters of DO3A-(gly)₃ or DO2A-(gly)₂ with 3-bromoacetamidoquinoline followed by quaternarization of the quinoline N atom with methyl triflate (synthetic details are given in the Supporting Information, Schemes S1–S3).

The ¹H NMR spectra of the Eu^{3+} -(**1**) and Eu^{3+} -(**2**) in D₂O showed a resonance at 25 ppm characteristic of four *H4* macrocyclic protons in Eu^{3+} complexes of this type that exist in solution in a square antiprism (SAP) coordination geometry as the major isomer (Supporting information, Figure S1).^{7,11} Non-enzymatic reduction of the quinolinium moiety of Eu^{3+} -(**1**) occurred rapidly after addition of one equivalent of β -NADH (pH 7) resulting in the formation of the reduced form of the complex (Supporting information Figure S2).¹⁵ Other reducing agents such as $\text{Na}_2\text{S}_2\text{O}_4$ and NaBH_4 also reduced the quinolinium moiety in the Eu^{3+} -(**1**) resulting in a similar change in CEST.^{16,17} In analogy to NADH model compounds, we suggest that the quinolinium ring on the pendant arm of the DOTA scaffold is reduced predominantly to the 1,4-dihydroquinoline derivative, even though we could not establish the structure of the reduced products unequivocally.¹⁵ Interestingly, the Eu^{3+} complex, in which the quinoline N-atom is not methylated does not undergo reduction by β -NADH and shows no change in the CEST (Supporting Information Figure S3). This observation indicates that the quaternary nitrogen of the quinolinium ring is essential for reduction to occur. The CEST signal arising from exchange of the Eu^{3+} -bound water molecule in Eu^{3+} -(**1**) increased in intensity somewhat, became sharper (indicative of slower exchange) and shifted from 48 ppm to 53 ppm upon reduction. The bound water life-times (τ_M) of the oxidized and reduced form estimated by fitting the experimental CEST spectra to the Bloch equations modified for exchange were 78 μs and 130 μs , respectively. In comparison, the τ_M of the parent $\text{Eu}[\text{DOTA}(\text{gly})_4]^-$ agent is about 160 μs . One can conclude then that substitution of aminoquinoline for a single glycine on the sidearm of $\text{DOTA}(\text{gly})_4$ results in about a two fold increase in the water exchange rate in the resulting Eu^{3+} complexes. It is worth noting that the slower water exchange rate of the reduced form is somewhat counterintuitive as one might have anticipated the oxidized species to have slower water exchange due to the presence of the more electron withdrawing positively charged methylquinolinium moiety.¹¹

The reaction of Eu^{3+} -(**2**) with two equivalents of β -NADH in water at pH 7 also gave a reduced complex. Interestingly, the CEST signal increased in intensity much more

dramatically in $\text{Eu}^{3+}\text{-}(2)$ (from 2% to 15 %) upon reduction than that observed previously for $\text{Eu}^{3+}\text{-}(1)$. The CEST peak of $\text{Eu}^{3+}\text{-}(2)$ also displayed a larger 7 ppm shift (from 43 to 50 ppm, see Figure 2). As expected, the water exchange lifetime of the reduced form of $\text{Eu}^{3+}\text{-}(2)$ (90 μs) was found to be significantly shorter than that in reduced $\text{Eu}^{3+}\text{-}(1)$. The τ_M for the oxidized form could not be determined due to the small magnitude of the CEST effect even at high B_1 power but its broad width indicates that water exchange was faster in the oxidized form of $\text{Eu}^{3+}\text{-}(2)$ than in $\text{Eu}^{3+}\text{-}(1)$.

The redox properties of these complexes were examined by cyclic voltammetry. Two well separated redox peaks corresponding to the two electron reduction of the quinolinium ring to the dihydroquinoline were detected for $\text{Eu}^{3+}\text{-}(1)$. The redox couple however, appeared to be quasi-reversible since the reduced form is not completely oxidized when an anodic current is applied. It is likely that the fully reduced dihydroquinoline derivative or its precursor species are susceptible to degradation in aqueous solutions and the incomplete oxidation during the anodic scan is due to the partial decomposition of the reduced derivative. $\text{Eu}^{3+}\text{-}(2)$ displayed a similar cyclic voltammogram under identical experimental conditions (Supporting Information Figure S5). In addition, this behavior was also seen in the cyclic voltammogram of the free ligand (2) indicating that the redox reaction occurs at the quinolinium moiety and the Eu^{3+} ion is not involved in the redox reaction.¹⁸

While CEST from the exchanging water molecule is generally independent of pH,⁶ the CEST signal of $\text{Eu}^{3+}\text{-}(1)$ showed a surprisingly strong pH-sensitivity (Figure 3). The bound water CEST peak at 48 ppm gradually broadened and decreased in intensity when the pH was increased from 5 to pH 8 (Figure 3 inset). Although the exact mechanism of this pH-responsiveness is yet unknown, the broadening of the CEST peak at higher pH suggests that this effect may be due to the base catalyzed deprotonation of the amide NH attached to the strongly electron withdrawing quaternarized quinoline ring, which in turn accelerates water exchange rate. This assumption is supported by the fact that the CEST signal of non-methylated form of $\text{Eu}^{3+}\text{-}(1)$ showed only negligible pH-dependence over the same pH range. The pH-dependent CEST is an interesting feature of $\text{Eu}^{3+}\text{-}(1)$ and may provide ideas for the design of future pH responsive agents. In comparison, $\text{Eu}^{3+}\text{-}(1)$ after reduction with $\beta\text{-NADH}$ did not show a significant pH responsive behavior.

To demonstrate that the oxidized and reduced forms can be distinguished by MRI, CEST imaging of a phantom containing the oxidized and reduced species (generated by adding two equivalents of NADH) of $\text{Eu}^{3+}\text{-}(2)$ was performed. The images were collected at 9.4 T using a modified fast spin echo sequence at 298 K. A 10 μT saturation pulse was applied for 3 s prior to collection of the image. The CEST images were generated by subtracting the saturation-on image from the saturation-off image. In agreement with the CEST spectra, the tube containing the reduced form showed the highest image intensity in the difference images compared to that of the oxidized form (Figure 4).

In conclusion, we report here the first activatable PARACEST redox sensor. We have incorporated an NAD^+/NADH analog, N-methylated quinolinium moiety as redox active functional group onto the pendant arm of the DOTA-tetraamide scaffold. The CEST signal of $\text{Eu}^{3+}\text{-}(2)$ with two quinolinium moieties was nearly completely silent while in the oxidized form, but “turns on” upon reduction with $\beta\text{-NADH}$. This makes $\text{Eu}^{3+}\text{-}(2)$ a good candidate for further development as an responsive redox sensor. The CEST signal of the Eu^{3+} -complex containing only one quinolinium group was much less redox responsive but showed an unexpected sensitivity to pH over the physiologically relevant pH range.

Supplementary Material

Refer to Web version on PubMed Central for supplementary material.

Acknowledgments

The authors acknowledge partial financial support for this work from the National Institutes of Health (CA-115531, CA-126608, RR-02584, and EB-00482) and the Robert A. Welch Foundation (AT-584).

References

1. Stryer, L. *Biochemistry*. 3. Freeman and co; New York: 1988.
2. Tu C, Nagao R, Louie AY. *Angewandte Chemie, International Edition*. 2009; 48:6547–6551. S6547/1–S6547/13.
3. Raghunand N, Jagadish B, Trouard TP, Galons JP, Gillies RJ, Mash EA. *Magnetic Resonance in Medicine*. 2006; 55:1272–1280. [PubMed: 16700014]
4. Aime S, Botta M, Gianolio E, Terreno E. *Angewandte Chemie, International Edition*. 2000; 39:747–750.
5. Ward KM, Aletras AH, Balaban RS. *Journal of Magnetic Resonance*. 2000; 143:79–87. [PubMed: 10698648]
6. Viswanathan S, Kovacs Z, Green KN, Ratnakar SJ, Sherry AD. *Chemical Reviews (Washington, DC, United States)*. 2010; 110:2960–3018.
7. Zhang S, Winter P, Wu K, Sherry AD. *Journal of the American Chemical Society*. 2001; 123:1517–1518. [PubMed: 11456734]
8. Ratnakar SJ, Woods M, Lubag AJM, Kovacs Z, Sherry AD. *Journal of the American Chemical Society*. 2008; 130:6–7. [PubMed: 18067296]
9. Viswanathan S, Ratnakar SJ, Green KN, Kovacs Z, De Leon-Rodriguez LM, Sherry AD. *Angewandte Chemie, International Edition*. 2009; 48:9330–9333. S9330/1–S9330/21.
10. Mani T, Tircso G, Togao O, Zhao P, Soesbe TC, Takahashi M, Sherry AD. *Contrast Media & Molecular Imaging*. 2009; 4:183–191. [PubMed: 19672854]
11. Woessner DE, Zhang S, Merritt ME, Sherry AD. *Magnetic Resonance in Medicine*. 2005; 53:790–799. [PubMed: 15799055]
12. Gomez E, Miguel M, Jimenez O, De la Rosa G, Lavilla R. *Tetrahedron Letters*. 2005; 46:3513–3516.
13. Ostovic D, Lee ISH, Roberts RMG, Kreevoy MM. *Journal of Organic Chemistry*. 1985; 50:4206–11.
14. Mikata Y, Mizukami K, Hayashi K, Matsumoto S, Yano S, Yamazaki N, Ohno A. *Journal of Organic Chemistry*. 2001; 66:1590–1599. [PubMed: 11262101]
15. Creighton DJ, Hajdu J, Mooser G, Sigman DS. *J Amer Chem Soc*. 1973; 95:6855–7. [PubMed: 4147716]
16. Wong YS, Marazano C, Gnecco D, Das BC. *Tetrahedron Letters*. 1994; 35:707–10.
17. Bunting JW, Meathrel WG. *Tetrahedron Letters*. 1971:133–6.
18. Blaedel WJ, Haas RG. *Analytical Chemistry*. 1970; 42:918–27.

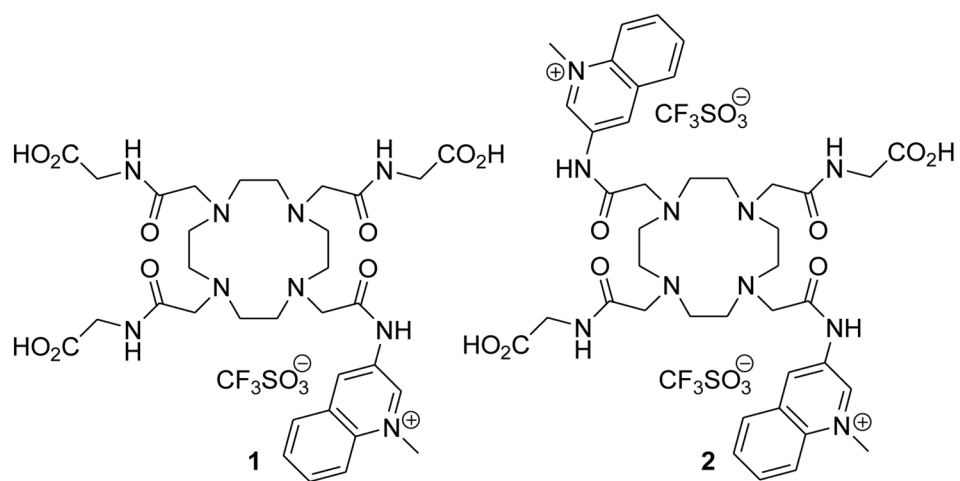


Figure 1.
Quinolinium DOTA tetraamide derivatives examined in this work.

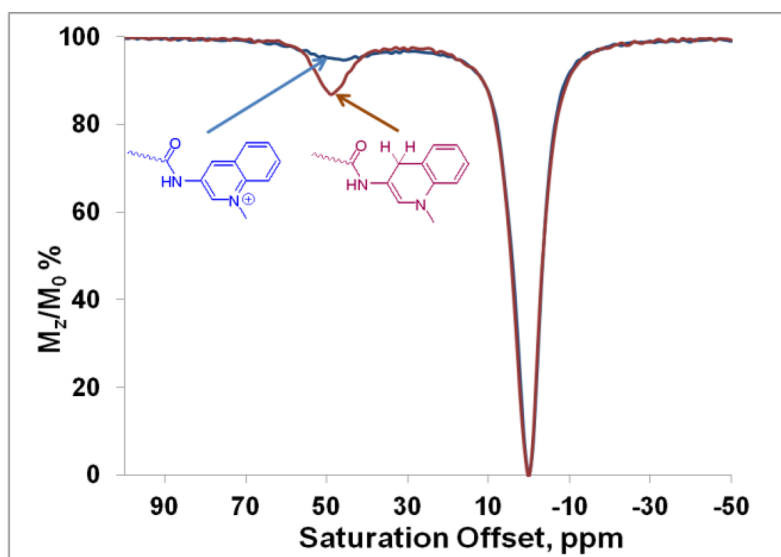


Figure 2. CEST spectra of the oxidized (blue) and reduced forms (red) of Eu^{3+} -(**2**) (20 mM) collected at 9.4 T, pH 7, 298 K, $B_1=10 \mu\text{T}$, with a presaturation time of 5 s.

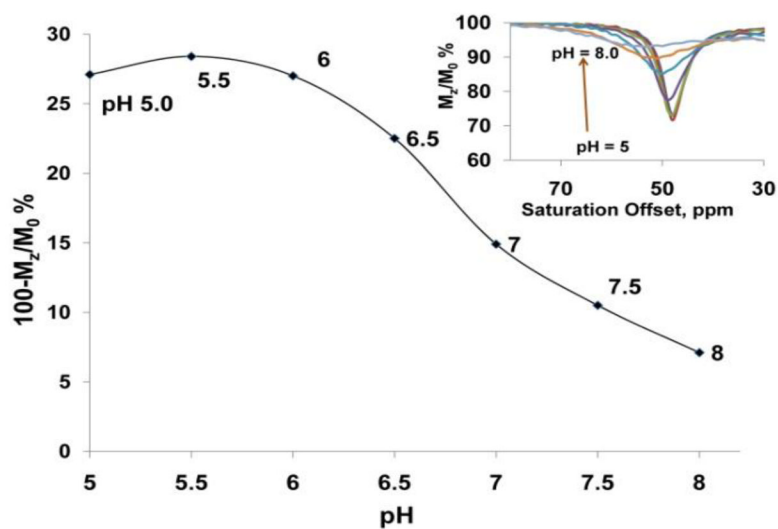


Figure 3. The pH dependence of the metal bound water CEST signal of Eu^{3+} -(**1**) (20 mM) at 9.4 T, 298 K, $B_1=10 \mu\text{T}$, and irradiation time of 5 s). The inset shows CEST spectra collected at each condition.

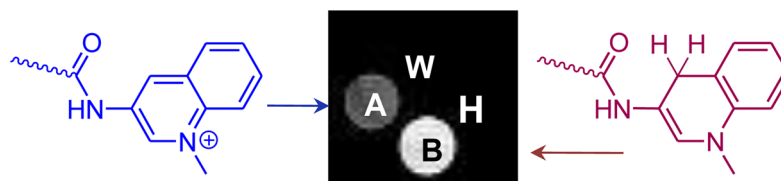


Figure 4. PARCEST images acquired for a phantom containing four tubes A: Eu^{3+} -**(2)** (20 mM) in HEPES buffer (pH 7, 0.25M); B: Eu^{3+} -**(2)** (20 mM) plus two equivalents of β -NADH in HEPES buffer (pH 7, 0.25M); W: water; H: HEPES buffer at pH 7.